available at www.sciencedirect.com

ScienceDirect

journal homepage: www.elsevier.com/locate/biochempharm

Characterization of IRA/IRB hybrid insulin receptors using bioluminescence resonance energy transfer

Christophe Blanquart [a,b], *Josepha Achi* [a,b], *Tarik Issad* [a,b,*]

[a] *Institut Cochin, Université Paris Descartes, CNRS (UMR 8104), Paris, France*
[b] *INSERM, U567, Paris, France*

ARTICLE INFO

Article history:
Received 10 April 2008
Accepted 7 July 2008

Keywords:
Insulin receptor isoforms
Insulin-like growth factor
Diabetes
Cancer
BRET

ABSTRACT

The insulin receptor (IR) is composed of two α-chains that bind ligands and two β-chains that possess an intracellular tyrosine kinase activity. The IR is expressed in cells as two isoforms containing or not exon 11 (IRB and IRA, respectively). Several mRNA studies have demonstrated that the two isoforms are co-expressed in different tissues and in several cancer cells. IRA/IRB hybrid receptors, constituting of an αβ-chain from IRA and an αβ-chain from IRB, are likely to occur in cells co-expressing both isoforms, but their study has been hampered by the lack of specific tools. In previous work, we used BRET to study IR and IGF1R homodimers and heterodimers. Here, we have used BRET to characterize IRA/IRB hybrids. BRET saturation experiments showed that IRA/IRB hybrids are randomly formed in cells. Moreover, by co-transfecting HEK-293 cells with a luciferase-tagged kinase-dead version of one isoform and a wild-type untagged version of the other isoform, we showed that IRA/IRB hybrids can recruit, upon ligand stimulation, a YFP-tagged intracellular partner. Finally, using BRET, we have studied ligand-induced conformational changes within IRA/IRB hybrids. Dose-response experiments showed that hybrid receptors bind IGF-2 with the same affinity than IRA homodimers, whereas they bind IGF-1 with a lower affinity. Altogether, our data indicate that IRA/IRB hybrid receptors can form in cells co-expressing both IR isoforms, that they are capable of recruiting intracellular partners upon ligand stimulation, and that they have pharmacological properties more similar to those of IRA than those of IRB homodimers with regards to IGF-2.

1. Introduction

The insulin receptor (IR) is a transmembrane tyrosine kinase receptor implicated in the regulation of energy metabolism. The IR is composed of two extracellular α-chains that bind ligands and two transmembrane and intracellular β-chains that possess the tyrosine kinase activity. The gene coding for IR is localized on chromosome 19 [1] and is composed of 22 exons [2]. Alternative mRNA splicing results in the expression of two isoforms containing or not the exon 11 (IRB and IRA, respectively) [3]. The exon 11 encodes for 12 amino acids localized at the C-terminal part of the α-chain. A functional consequence of the deletion of these 12 amino acids is a modification of the receptor pharmacology. Indeed, the affinity of insulin for IRA is higher than the affinity of insulin for IRB [4]. Moreover, it has been shown that IGF-2 (insulin-like growth factor-2) binds to IRA, but not to IRB, with an affinity close to that of insulin [5]. The expression profile of these two isoforms is different. Both isoforms are expressed in insulin sensitive tissues (liver, muscles and adipocytes) [3,4].

* *Corresponding author at*: Institut Cochin, Université Paris Descartes, CNRS (UMR 8104), Paris, France. Tel.: +331 40 51 64 09; fax: +331 40 51 64 30.
E-mail address: issad@cochin.inserm.fr (T. Issad).
0006-2952/$ – see front matter
doi:10.1016/j.bcp.2008.07.027

However, IRA is highly expressed in fetal tissues where it seems to have a major function in embryonic development [5]. Interestingly, changes in the IRB to IRA mRNA ratio have been observed in tissues of diabetic patients [6–9]. Moreover, in a number of tumors, over-expression of IRA has been observed [10–12].

Several studies have demonstrated the existence of hybrid receptors constituting of an αβ-chain from the IR and an αβ-chain from IGF1R [13]. IGF1R/IR hybrids bind IGF-1 and IGF-2 with high affinity but bind insulin with a relatively low affinity [14]. The formation of these hybrid receptors is believed to occur randomly in the endoplasmic reticulum during their biosynthesis [11,15]. Indeed, the formation of these hybrids at the cell surface depends on the relative expression level of each type of receptor [11]. Increased presence of these hybrid receptors at the cell surface has been demonstrated in pathologies such as diabetes and cancers [11,16–18]. It has been suggested that these hybrid receptors could participate in insulin resistance in type II diabetes by decreasing the number of insulin binding sites [17,18]. Moreover, the increased proportion of hybrid receptors may result in an increase in binding sites for IGF-1 and IGF-2 and participate in signalling by these growth factors in cancer [11].

IR and IGF1R possess only 60% homology whereas IRA and IRB are more than 99% identical. Since hybrid receptors can be formed between IR and IGF1R, IRA/IRB hybrid receptors are also likely to occur in cells co-expressing the two isoforms of the IR. However, the demonstration of the existence and the study of these IRA/IRB hybrids are hampered by the lack of biochemical tools such as antibodies specifically directed against each isoform. We previously showed that BRET technology can be used to study insulin [19] and IGF-1 [20] receptors as well as IRA/IGF1R hybrid receptors [21]. In the present study, we have used BRET to determine (i) whether IRA/IRB hybrid receptors can form in cells co-expressing both isoforms and (ii), whether IRA/IRB hybrid receptors have specific properties compared to homodimers of each type. We show that the formation of IRA/IRB hybrid receptors can indeed occur in cells co-expressing both isoforms of the IR and that their pharmacological properties are more similar to IRA homodimer with regards to IGF-2, whereas they resemble IRB with regards to IGF-1.

2. Materials and methods

2.1. Reagents

All reagents have been described previously [19,20,22,23]. Briefly, insulin (Umuline) was from Lilly France SA. IGF-1, IGF-2, wheat germ lectin agarose and *N*-acetylglucosamine were from Sigma–Aldrich (Saint-Quentin Falavier, France). Coelanterazine was purchased from interchim (Montluçon, France).

2.2. Expression vectors

Expression vectors for IRA (IRA, IRA-Rluc, IRA_{KD}-Rluc and IRA-YFP), for IRB (IRB, IRB-Rluc, IRB_{KD}-Rluc and IRB-YFP) and for YFP-PTP1B-D181A-Cter have been described previously [20–22,24]. The YFP-p52Shc expression vector was obtained as follows: p52Shc insert was prepared by PCR on pcDNA3 p52Shc (rat) using the following Oligonucleotides: forward: 5′ GGGAAGATCTAACAAGCTGAGTGGAGGCGGCGG 3′, reverse: 5′ CCGGAATTCCTCACACTTTTCGATCCACAGGT 3′. The PCR product was digested with Bgl II and EcoR I (restriction sites present in the oligonucleotides) and cloned in pEYFP-C1 digested with Bgl II and EcoR I.

2.3. Cell culture, transfection, and partial purification of tyrosine kinase fusion proteins

HEK-293 cells maintained in Dulbecco's Modified Eagles's Medium (DMEM, Invitrogen, Cergy Pontoise, France) supplemented with 4.5 g/l glucose and 10% fetal bovine serum (Eurobio, Les Ulis, France) were seeded at a density of 2.5×10^5 cells/35 mm dish. Transient transfections were performed 1 day later using FuGENE 6 (Roche Diagnostics, Indianapolis, IN) according to the manufacturer's protocol. For BRET saturation experiments, HEK-293 cells were transfected with 0.6 μg of Rluc-fused IR cDNA and increasing amounts of YFP-fused IR cDNA (0.05–2 μg). At the end of the experiments, YFP expression level was determined by measuring fluorescence emission at 530 nM, after illumination at 485 nM.

For the study of YFP-PTP1B-D181A-Cter and YFP-p52Shc interaction with hybrid receptors, HEK-293 cells were transfected with 0.6 μg of IRB_{KD}-Rluc cDNA or 0.6 μg of IRA $_{KD}$-Rluc cDNA, 0.3 μg of YFP-PTP1B-D181A-Cter cDNA or 0.3 μg of YFP-p52Shc cDNA and either 0.3 μg of IRB (untagged) cDNA or 0.3 μg of IRA (untagged) cDNA per 35 mm dish. One day after transfection, cells were transferred into 96-well microplates (Viewplate, PerkinElmer, Courtaboeuf, France) at a density of 3×10^4 cells/dish. The following day, BRET measurements were performed as described below.

For the study of conformational changes within homodimeric or hybrid receptors in intact cells, HEK-293 cells were transfected with 0.3 μg of Rluc-fused IR cDNA and 0.3 μg of YFP-fused IR cDNA per 35 mm dish.

For partial purification of IR fusion proteins, cells were co-transfected with 0.45 μg of Rluc-fused IR cDNA and 0.45 μg of YFP-fused IR cDNA per 35 mm dish. Two days after transfection, fusion proteins were purified by Wheat Germ Lectin (WGL) chromatography as described previously [19,20]. After elution with N-acetylglucosamine (0.3 M), fractions enriched in Rluc activity were pooled, aliquoted and stored at −80 °C for subsequent use.

2.4. BRET measurements

All BRET measurements were performed at room temperature using the FusionTM microplate analyzer (PerkinElmer). BRET measurements on partially purified receptors were performed in a total volume of 50 μl containing 0.02% Triton X100, 4 mM MOPS (pH 7.4), 10 μl (approximately 4 μg of proteins/μl) of concentrated WGL-eluate, and ligands. After 15 min of pre-incubation at room temperature, the substrate of luciferase (coelanterazine) was added to the preparation at a final concentration of 5 μM. Light emission acquisition (at 480 and 530 nm) was then started immediately using the Fusion microplate analyzer. For the study of conformational changes within receptors in intact cells, cells were pre-incubated for

15 min in PBS in the presence of 2.5 μM coelenterazine. Ligands were then added and light-emission acquisition at 485 and 530 nm was started immediately. For the study of the interaction between receptors and intracellular partners, cells were also pre-incubated for 15 min in the presence of 2.5 μM coelenterazine. Ligands were then added and the dynamics of the interaction between the receptors and intracellular partners was monitored during at least 20 min following ligand addition. BRET measurements were performed every 1.5–2 min (the interval of time between two measurements for a given well depending on the number of experimental conditions analyzed in the experiment). Each measurement corresponded to the signal emitted by the whole population of cells present in a well. BRET signal was expressed in milliBRET Unit (mBU). The BRET unit has been defined previously as the ratio 530/485 nm obtained when the two partners are present, corrected by the ratio 530/485 nm obtained under the same experimental conditions, when only the partner fused to *Renilla* luciferase is present in the assay [19,22,25]

2.5. Statistical analysis

Data are expressed as the means ± S.E.M. of at least three experiments. For the BRET experiments, the statistical comparisons were made using two-tailed student's *t* test for paired values. To compare EC_{50}, we used the two-tailed Student's *t* test for unpaired values.

3. Results

3.1. Study of IRA/IRB hybrid receptor formation by BRET

The demonstration of the formation of IRA/IRB hybrid receptors has been hampered by the lack of tools such as antibodies specifically directed against the IR isoforms. In previous work, we showed that it is possible to specifically study IR and IGF1R homodimers as well as IRA/IGF1R heterodimers by BRET [19–21]. Here, we applied this technology to specifically detect the formation of IRA/IRB hybrid receptors and to evaluate the propensity of each IR isoform to form homodimers and heterodimers. To this aim, we used BRET saturation experiments, which have been developed by several groups to evaluate the relative affinity between two partners [23,26–28]. HEK-293 cells were transfected with a fixed amount of cDNA coding for Rluc-fused IR and increasing amounts of cDNA coding for YFP-fused IR. BRET values were measured 48 h after transfection and were expressed as a function of the YFP/luciferase ratio (YFP/Rluc). The curves obtained were hyperbolic and reached an asymptote ($BRET_{max}$) (Fig. 1). In contrast to the

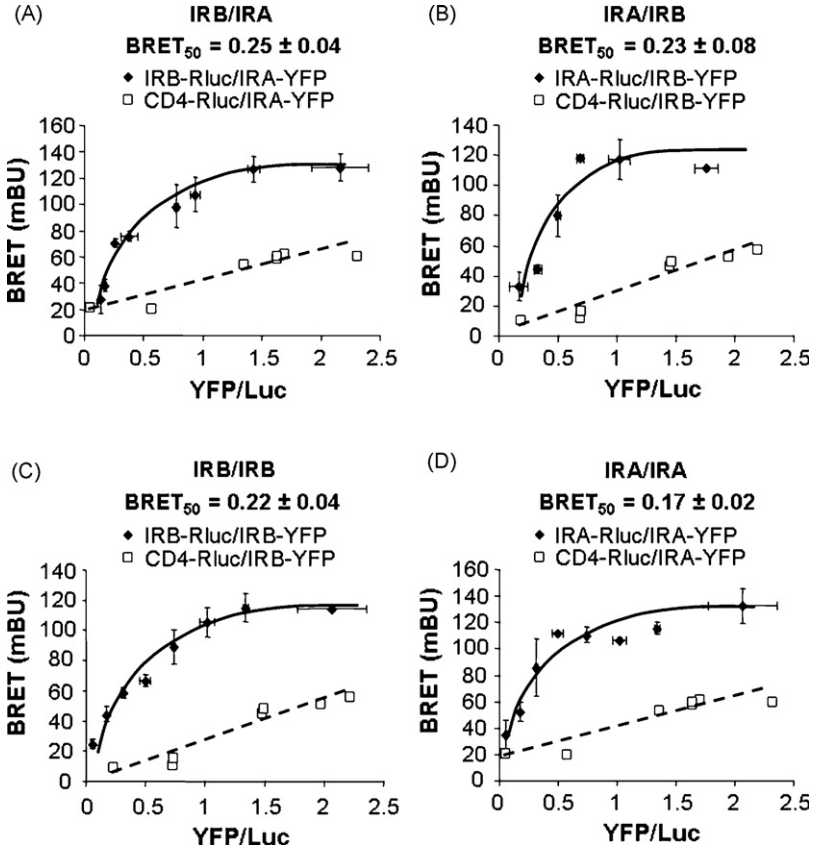

Fig. 1 – BRET saturation curves for homodimeric and hybrid receptor formation. HEK-293 cells were co-transfected with a fixed amount of cDNA coding for IR-Rluc (or CD4-Rluc as a negative control) and increasing amounts of cDNA coding for IR-YFP. BRET and total fluorescence were measured 48 h after transfection. Results are expressed as the mean ± S.E.M. of at least three independent experiments. The curves were fitted using a non-linear regression equation assuming a single binding site.

hyperbolic curves obtained for IR-Rluc/IR-YFP BRET pairs, BRET values measured between IR-YFP and the irrelevant partner CD4-Rluc were much weaker and increased linearly with YFP/Rluc ratio. This weaker, non-saturable BRET signal probably corresponded to random, non-specific collisions between IR-YFP and CD4-Rluc in the membrane bi-layer, and contrasted with the saturable, specific BRET obtained with IR-Rluc and IR-YFP isoforms. The YFP/Rluc ratio that gives half of the $BRET_{max}$ ($BRET_{50}$) reflects the relative affinity between the two partners. If the propensity to form homodimers were higher than propensity to form heterodimers, we should obtain a lower $BRET_{50}$ for homodimers than for heterodimers. Indeed, if the propensity to form homodimers were higher, much more IR-YFP acceptor molecules will be needed to engage half of the IR-Rluc donnor molecules ($BRET_{50}$), since IR-Rluc will tend to dimerize with IR-Rluc rather than with IR-YFP. Saturation curves obtained for the different combination of receptors all show similar $BRET_{50}$ values (IRB-RLuc/IRA-YFP: $BRET_{50} = 0.25 \pm 0.04$; IRA-Rluc/IRB-YFP: $BRET_{50} = 0.23 \pm 0.08$; IRB-RLuc/IRB-YFP: $BRET_{50} = 0.22 \pm 0.04$; IRA-Rluc/IRA-YFP: $BRET_{50} = 0.17 \pm 0.02$). These results suggest that IRA/IRB hybrid receptors should form with the same probability as homodimers of each type.

HEK-293 cells only express the endogenous IRA receptors, in agreement with their embryonic origin (Supplementary Fig. S1). These endogenous IRA receptors are functional in terms of insulin-induced autophosphorylation (Supplementary Fig. S2-A), In HEK-293 cells transfected with IRB-YFP, endogenous IRA receptors could be co-immunoprecipitated with IRB-YFP receptor using an anti-GFP antibody (Supplementary Fig. S2-B), supporting the notion that IRA/IRB hybrids are likely to occur in cells co-expressing both isoforms. Moreover, IRA-Rluc/IRB-YFP and IRB-Rluc/IRA-YFP hybrid receptors can also be formed in an other cell type, as demonstrated by specific BRET measured in the cancer-derived MCF-7 cells (Supplementary Fig. S3).

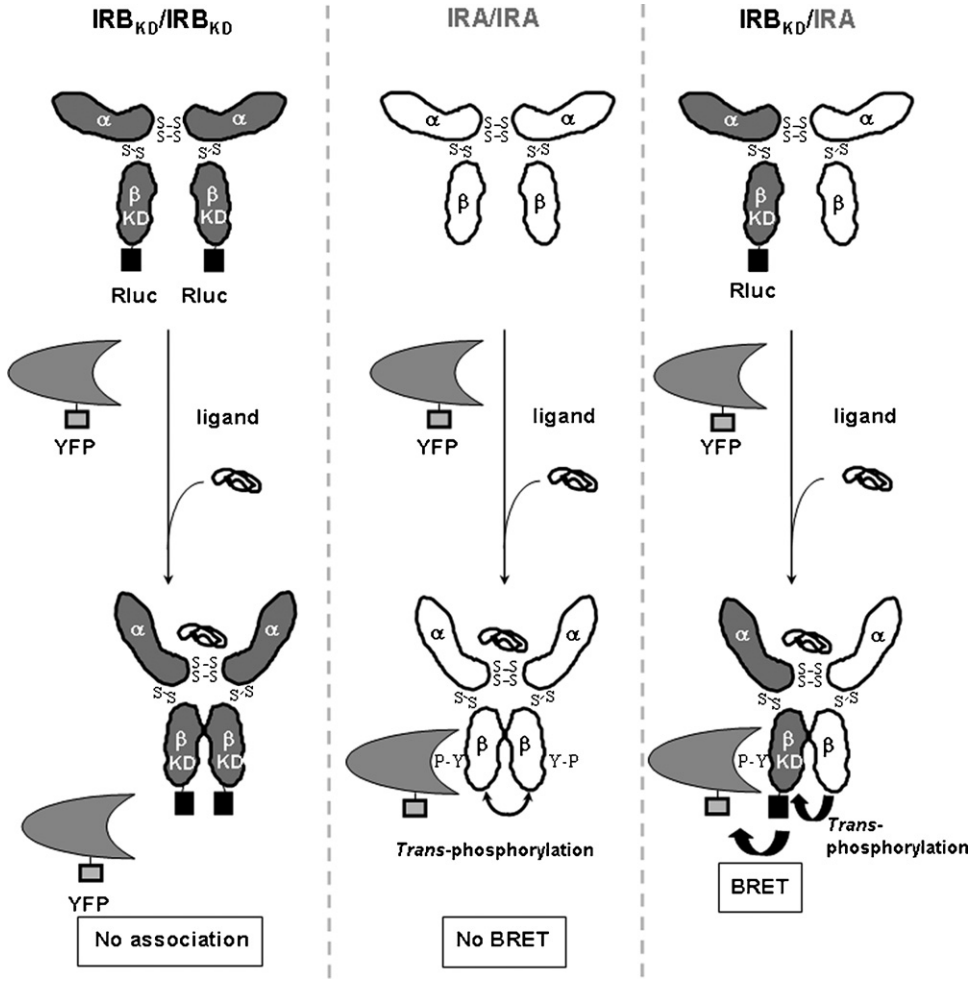

Fig. 2 – Principle of a BRET-based assay to monitor ligand-induced recruitment of an intracellular partner by IRA/IRB hybrid receptors in intact cells. In HEK-293 cells, co-transfection with an intracellular partner fused to YFP, IRB_{KD}-Rluc and wild-type IRA is likely to result in the formation of IRB_{KD}-Rluc/IRB_{KD}-Rluc and IRA/IRA homodimers, and IRB_{KD}-Rluc/IRA hybrids. IRB_{KD}-Rluc/IRB_{KD}-Rluc cannot autophosphorylate and therefore cannot recruit the YFP-fused intracellular partner. IRA/IRA receptors can autophosphorylate and recruit the YFP-fused intracellular partner but cannot produce a BRET signal. In IRB_{KD}-Rluc/IRA hybrid receptors, the IRA β-subunit can *trans*-phosphorylate the IRB_{KD}-Rluc β-subunit in presence of ligands, which can then recruit the YFP-fused intracellular partner and produce a BRET signal.

3.2. *IRA/IRB hybrid receptors are capable of recruiting intracellular partner following ligand induction*

In a previous study, we demonstrated that the interaction of an intracellular partner with the IGF1R/IRA hybrid receptor can be measured by BRET [21]. Indeed in HEK-293 cells co-transfected with a kinase-defective (KD) mutant of IGF1R fused to Rluc, an untagged IRA and a YFP-tagged interacting partner (YFP-PTP1B-D181A-Cter, a soluble substrate trapping mutant of PTP1B) [21], only the $IGF1R_{KD}$-Rluc/IRA hybrid receptors produced a BRET signal in response to ligands [21]. This signal reflects the fact that ligands stimulate the *trans*-phosphorylation of the $IGF1R_{KD}$-Rluc β-chain by the IRA β-chain, thereby inducing the recruitment of the YFP-tagged interacting partner. In the current work, we have co-transfected HEK-293 cells with IRB_{KD}-Rluc, untagged IRA,

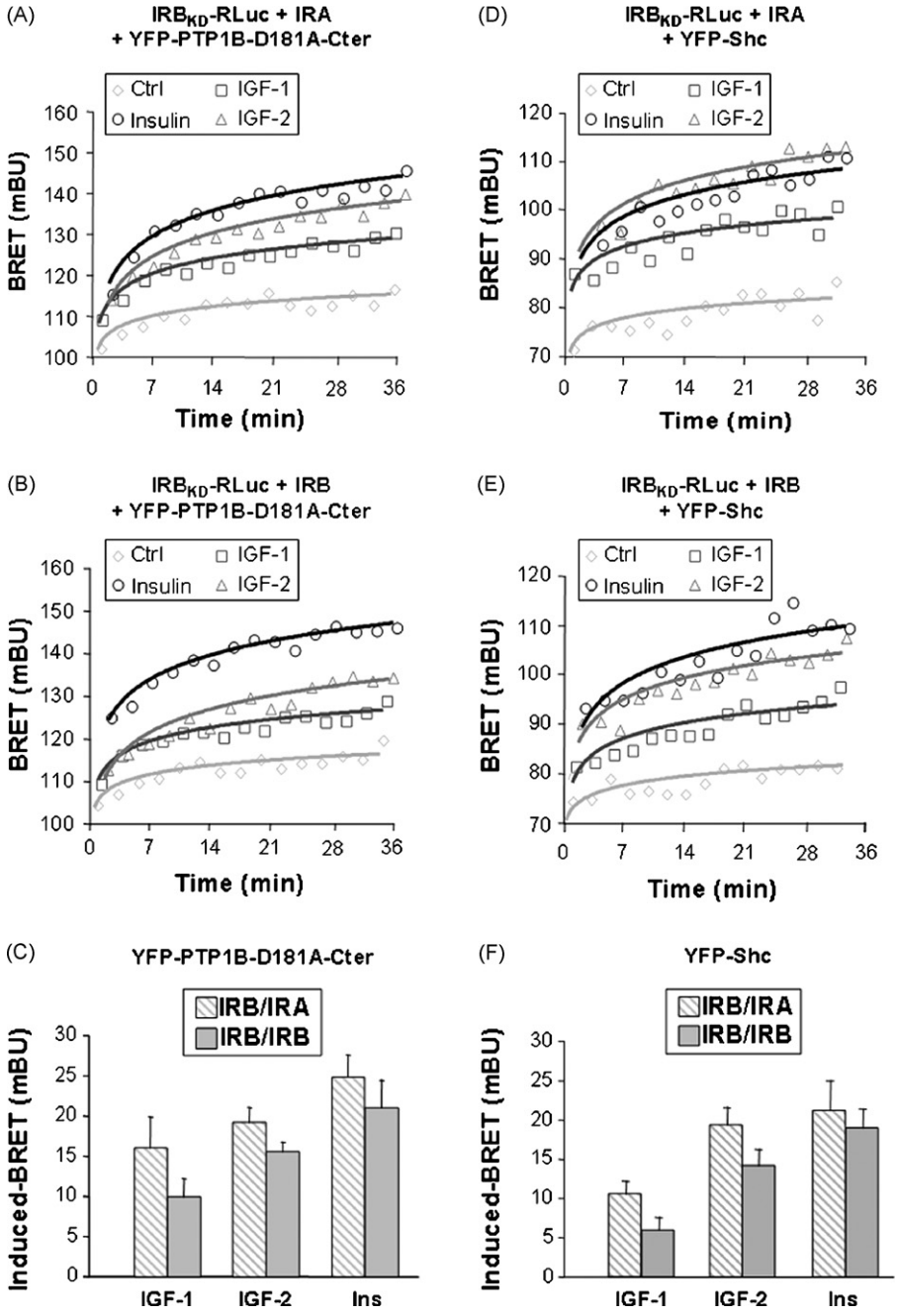

Fig. 3 – Ligand-induced interaction of IRB_{KD}-Rluc/IRA hybrid receptors with YFP-PTP1B-D181A-Cter and YFP-p52Shc. HEK-293 cells were transfected with IRB_{KD}-RLuc, IRA (A and D) or IRB (B and E) and YFP-PTP1B-D181A-Cter (A and B) or YFP-p52Shc (D and E). BRET was measured in real time, in intact living cells, after addition of 100 nM of IGF-1, IGF-2 or insulin. Representative experiments are shown (A, B, D, and E). (C and F) Graphic representation of ligand-induced BRET signal (BRET above basal) measured 20 min after addition of 100 nM of IGF-1, IGF-2 or insulin (results are the means ± S.E.M. of three independent experiments).

and either YFP-PTP1B-D181A-Cter or YFP-p52Shc as intracellular partner (Fig. 2). Fig. 3A shows that upon ligand binding, IRB_{KD}-Rluc/IRA receptors can produce a BRET signal corresponding to the recruitment of YFP-PTP1B-D181A-Cter to hybrid receptors. The BRET produced by the hybrids upon ligand binding was similar to the BRET produced by their homodimeric counterparts (IRB_{KD}-Rluc/IRB-YFP) (Fig. 3B and C). Fig. 3D shows the interaction between hybrid receptors and p52Shc, a well-known intracellular partner of IR. We observed that IRB_{KD}-Rluc/IRA hybrids can interact with p52Shc and produce a ligand-induced BRET similar to IRB_{KD}-Rluc/IRB (Fig. 3D–F). Similar results were obtained when studying IRA_{KD}-Rluc/IRB (Fig. 4). These results demonstrate that when IRA and IRB are co-expressed in a cell, IRA/IRB hybrids are present at the cell surface and can transmit intracellular signals by recruiting interacting partners.

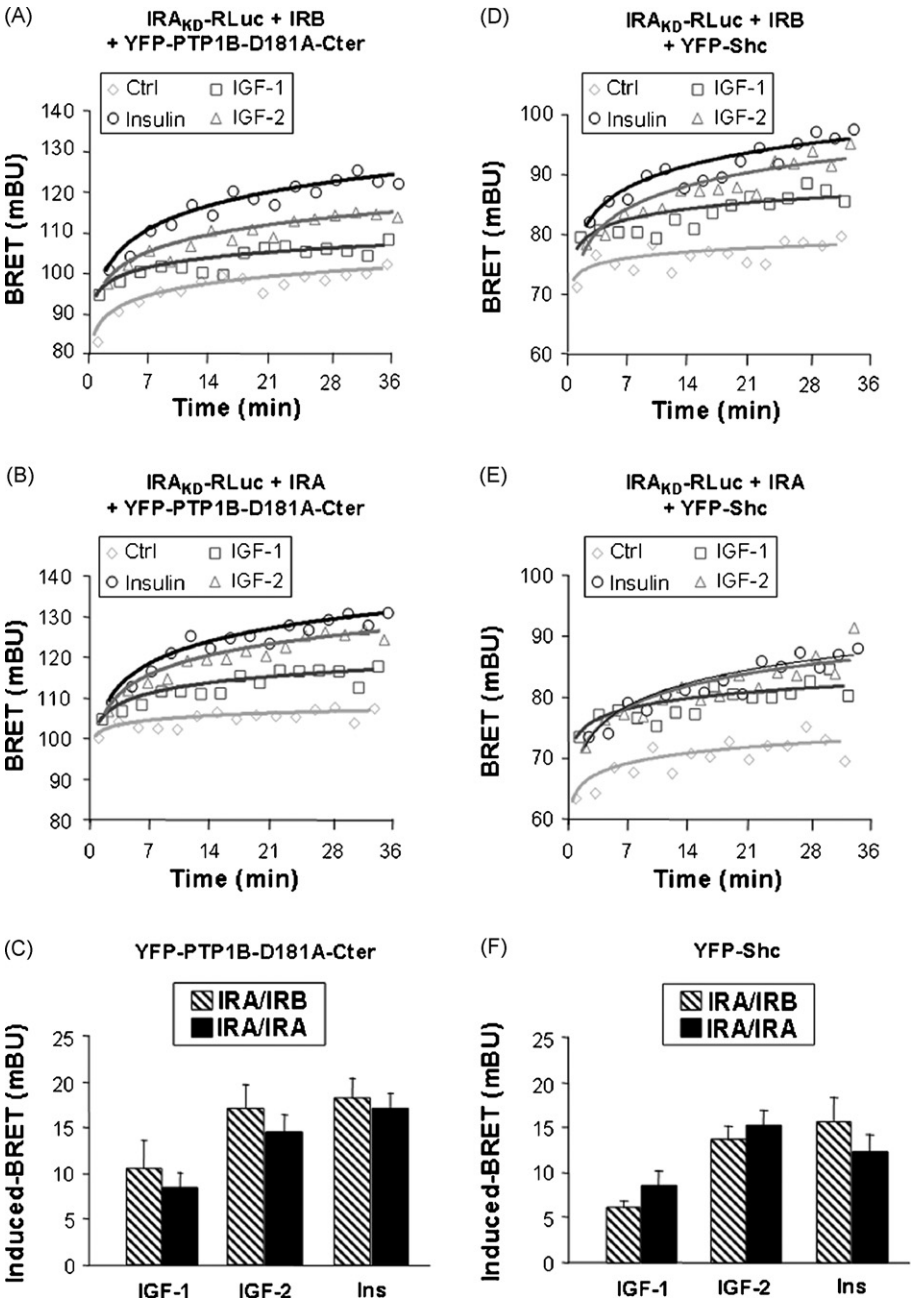

Fig. 4 – Ligand-induced interaction of the IRA_{KD}-Rluc/IRB hybrid receptors with YFP-PTP1B-D181A-Cter and YFP-p52Shc. HEK-293 cells were transfected with IRA_{KD}-RLuc, IRB (A and D) or IRA (B and E) and YFP-PTP1B-D181A-Cter (A and B) or YFP-p52Shc (D and E). BRET was measured in real time, in intact living cells, after addition of 100nM of IGF-1, IGF-2 or insulin. Representative experiments are shown (A, B, D, and E). (C and F) Graphic representation of ligand-induced BRET signal (BRET above basal) measured 20 min after addition of 100 nM of IGF-1, IGF-2 or insulin (results are the means ± S.E.M. of three independent experiments).

3.3. Monitoring the activation state of IRA/IRB hybrid receptors

Binding of ligands to IR induces a conformational change which brings the two β-chains into proximity, allowing *trans*-phosphorylation of one β-subunit by the other. In previous studies, we showed that ligand-induced conformational change within IR and IGF1R homodimers as well as within IRA/IGF1R heterodimers can be measured by BRET [19–21]. In these studies, we observed that the ligand-induced BRET signal was very modest in intact cells, whereas a robust effect was measured on receptors partially purified by WGL chromatography. Similar results were obtained in the present study. Indeed, ligand-induced conformational changes within IRA/IRB hybrids in intact cells were very modest (Fig. 5). As observed previously [19–21], partial purification of the receptors markedly improves ligand-induced BRET signal (Fig. 6). We observed that insulin was the most effective ligand to induce BRET signal on IRB homodimers, whereas insulin and IGF-2 induced similar effects on IRA homodimers. The effect of IGF-2 was similar on IRA homodimers and on IRA/IRB hybrids, but seems to be lower on IRB homodimers (Fig. 6). Therefore, subtle differences between the different combinations of receptors appear to be detectable by this method even at high ligand concentrations (100 nM). This prompted us to study more precisely the pharmacology of the uncharacterized IRA/IRB hybrid receptors by performing dose-response experiments with the different ligands.

3.4. Dose-dependent effect of insulin, IGF-1 and IGF-2 on IRA/IRB hybrids

Partially purified hybrid receptors were incubated with increasing concentrations of insulin, IGF-1 and IGF-2. Ligand-induced BRET corresponds to the difference between basal BRET and BRET measured in the presence of ligand. Results are expressed as percentage of maximal ligand-induced BRET and plotted against ligand concentrations (Fig. 7). The EC_{50} obtained in these experiments are summarized in Table 1. The EC_{50} of insulin for homodimeric and heterodimeric receptors were similar (Fig. 7A). The EC_{50} of IGF-1 for IRB-Rluc/IRB-YFP, IRB-Rluc/IRA-YFP and IRA-Rluc/IRB-YFP could not be determined with accuracy, because a plateau could not be reached, even at the highest ligand concentrations (Fig. 7B). In any case, these EC50 were all higher than 50 nM. In contrast, the EC_{50} of IGF-1 for IRA-Rluc/IRA-YFP was 24.97 ± 0.17 nM and therefore seems to be substantially lower than for the other combinations of receptors (Fig. 7B, right panel). The EC_{50} of IGF-2 for homodimeric IRA and IRA/IRB hybrid receptors were similar (Fig. 7C, right panel). In contrast, the EC_{50} of IGF-2 for IRB-Rluc/IRB-YFP was equal to 24.95 ± 0.06 nM and was statistically higher than for the other combinations of receptors (Fig. 7C). These results indicate that the pharmacology of IRA/IRB hybrids for insulin is similar to homodimeric receptors. The sensitivity of IRA/IRB hybrids for IGF-1 seems to be similar to that of IRB/IRB homodimers. In contrast, the sensitivity of IRA/IRB hybrids to IGF-2 is higher than that of IRB homodimers and similar to that of IRA homodimers.

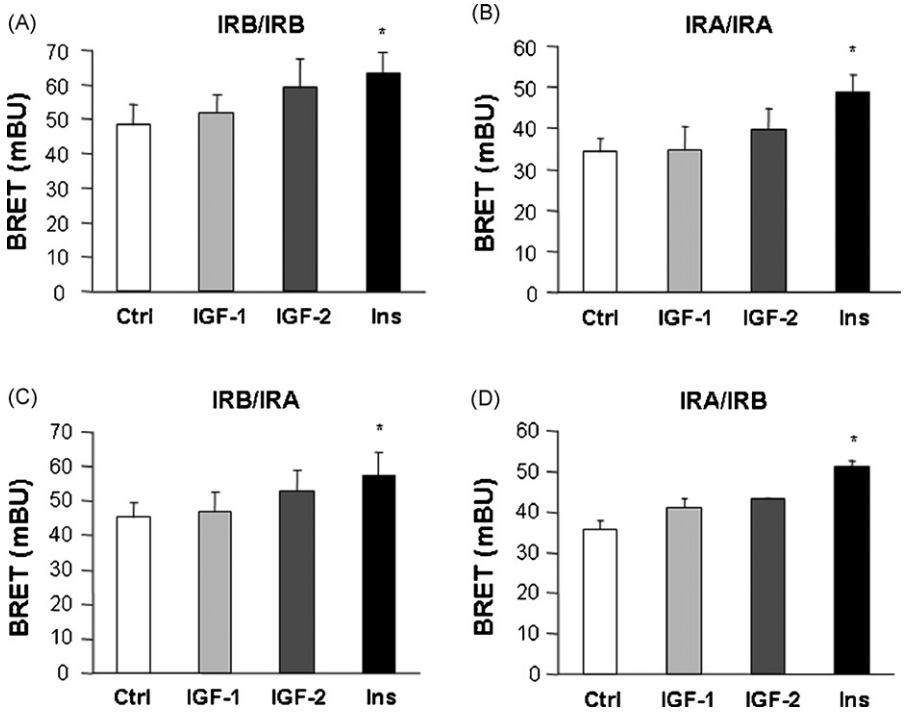

Fig. 5 – Effect of ligands on BRET signal in intact cells. HEK-293 cells were transfected with IRB-RLuc and IRB-YFP (A), IRA-Rluc and IRA-YFP (B), IRB-RLuc and IRA-YFP (C) or IRA-Rluc and IRB-YFP (D). BRET was measured in real time, in intact living cells, after addition of 100nM of IGF-1, IGF-2 or insulin. Results are the means ± S.E.M. of at least four independent experiments. *$p < 0.05$ when compared to unstimulated control.

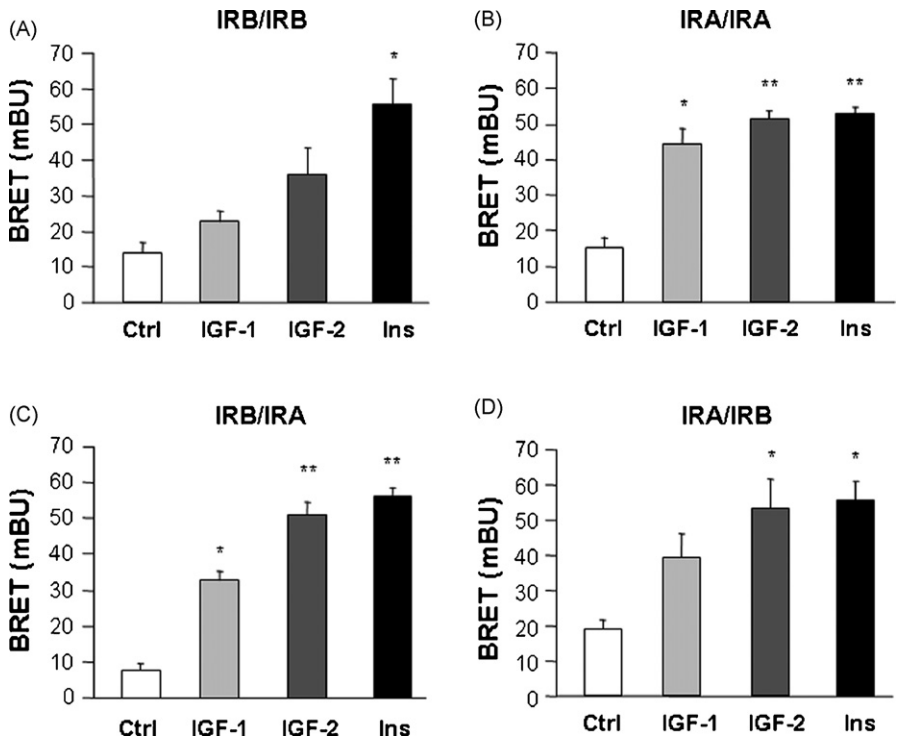

Fig. 6 – Effect of ligands on partially purified IRA/IRB receptors. HEK-293 cells were transfected with IRB-RLuc and IRB-YFP (A), IRA-Rluc and IRA-YFP (B), IRB-RLuc and IRA-YFP (C) or IRA-Rluc and IRB-YFP (D). Receptors were partially purified by WGL chromatography. BRET assays were performed by incubating partially purified receptors with 100 nM of IGF-1, IGF-2 or insulin as described in Section 2. Results are the means ± S.E.M. of at least four independent experiments. *$p < 0.05$; **$p < 0.01$ when compared to unstimulated control.

4. Discussion

The absence of exon 11 confers on IRA the ability to bind both insulin and IGF-2 with high affinity, whereas IRB only binds insulin with high affinity [5]. Hetero-dimerization of IR with IGF1R receptors has been demonstrated in cells co-expressing these two receptors. These heterodimers, composed of an αβ-chain from IR and an αβ-chain from IGF1R, bind IGF-1 and IGF-2 with high affinity, whereas they bind insulin with low affinity [4,14,29,30]. Because the homology between IRA and IRB is much higher than the homology between IR and IGF1R, we hypothesized that IRA/IRB hybrid receptors are very likely to occur in cells co-expressing both isoforms. In order to verify this hypothesis, we have used the BRET technology to study IRA/IRB hybrids.

In order to evaluate the propensity of IRA and IRB to form heterodimers, we have performed BRET saturation experiments using IR isoforms fused to Rluc or YFP. All the curves obtained were hyperbolic and reached a plateau, suggesting that the BRET signal measured corresponded to specific dimer formation between IR isoforms rather than to bystander interactions. Indeed, under similar experimental conditions, saturation could not be reached with a non-relevant plasma membrane Rluc-fused protein (CD4-Rluc). $BRET_{50}$ values, which reflect, in a BRET saturation assay, the relative affinity of one partner for the other, were similar whatever the isoform combination used (Fig. 1). This result strongly suggests that the probability of formation of IRA/IRB hybrid receptors is the same as the probability of formation of homodimeric receptors. A similar conclusion was reached for IR/IGF1R heterodimer formation using immunoprecipitation-based assays [11,15]. This suggests that an increase in the expression of one isoform will increase the quantity of homodimers of this isoform as well as the quantity of heterodimers, to the disadvantage of homodimers of the other isoform.

Functional studies of the IRA/IRB hybrid receptors are hampered by the lack of appropriate tools such as isoform specific antibodies. Moreover, even if such tools existed, these studies would remain difficult due to the concomitant expression of homodimers of each isoform in cells. In our previous work, we have shown that is possible to monitor the activation of IRA/IGF1R hybrid receptors in intact living cells by BRET [21], using a kinase-dead Rluc-tagged receptor and a YFP-tagged interacting partner. In this report, we also demonstrated, using a similar procedure, ligand-induced recruitment of PTP1B to IRA/IRB hybrid receptor. Moreover, we extended this procedure to another intracellular partner, p52Shc. The demonstration that p52Shc binds to IRA/IRB hybrids, in a ligand stimulated manner, indicates that these hybrids are indeed capable of transmitting an intracellular signal. Whereas PTP1B predominantly binds to the three phospho-tyrosines of the kinase domain, p52Shc is believed to bind to tyrosine 972 located on the juxtamembrane domain through its PTB domain. Although transphosphorylation of the tyrosine kinase of the IR has already been demonstrated [31], it had not been determined previously

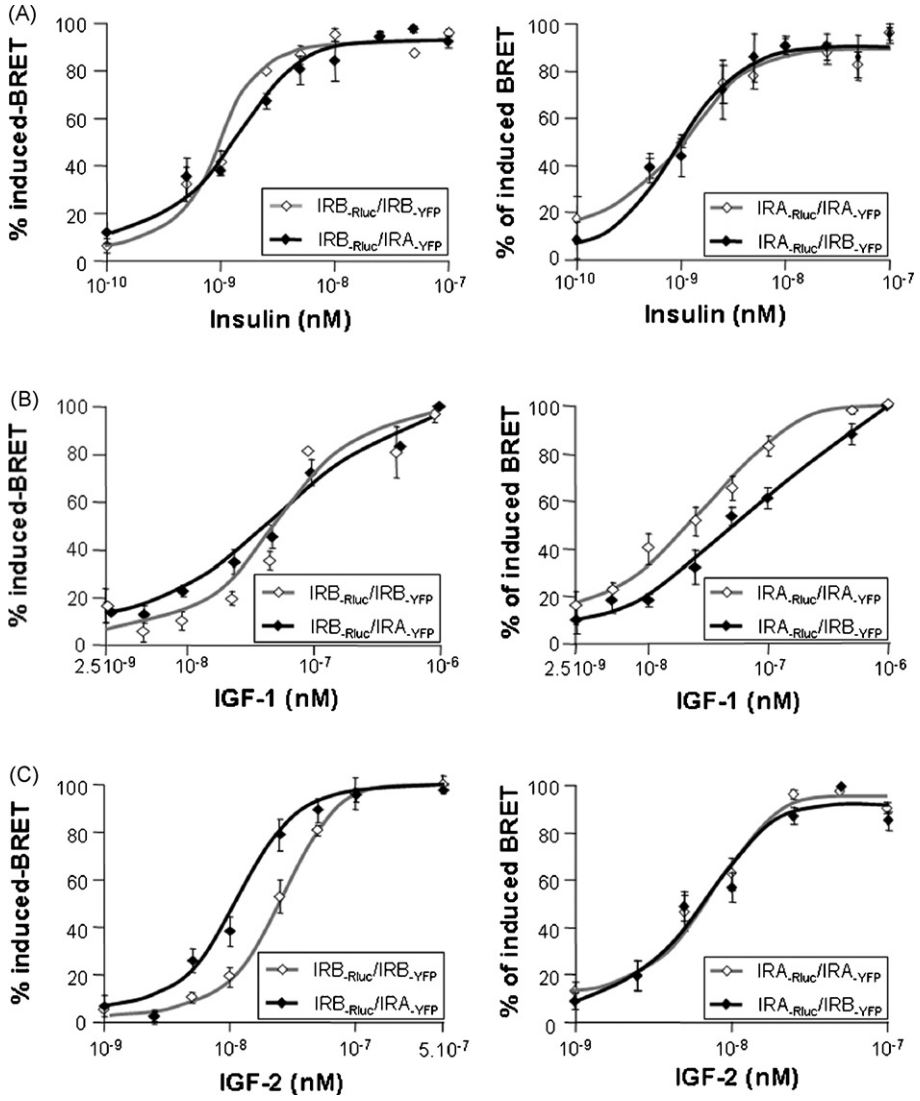

Fig. 7 – Dose-dependent effect of insulin, IGF-1 and IGF-2 on partially purified receptors. Receptors were partially purified from HEK-293 cells transfected with IRB-RLuc and IRB-YFP, IRA-Rluc and IRA-YFP, IRB-RLuc and IRA-YFP or IRA-Rluc and IRB-YFP. Partially purified receptors were incubated with increasing concentrations of insulin (A), IGF-1 (B) or IGF-2 (C). BRET signal was measured as described in Section 2. Dose response curves corresponded to ligand-induced BRET plotted against ligand concentration. Results are expressed as percent of maximal ligand-induced BRET in each experiment. Grey curves correspond to homodimeric receptors and black curves correspond to hybrid receptors. Results are the means ± S.E.M. of at least four independent experiments.

whether phosphorylation of tyrosine 972 occurs in *cis* or in *trans*. The fact that YFP-p52Shc produced a BRET signal with hybrid receptors (Figs. 3D–F and 4D–F) suggests that phosphorylation of tyrosine 972 indeed occurs in *trans*, the tyrosine 972 of the kinase-dead β-subunit being phosphorylated by the wild-type kinase of the other subunit.

We also evaluated the effects of ligands on these receptors by studying ligand-induced conformational changes within homodimers and heterodimers. The ligand-induced BRET signals were barely detectable in intact living cells, whereas partial purification of the receptors by WGL chromatography considerably improves this signal. Similar observations have already been made in our previous studies [19–21]. Several potential mechanisms may be responsible for the poor ligand-induced BRET signal in intact cells compared to partially purified insulin receptors. For instance, since BRET depends not only on the distance, but also on the relative orientation of the BRET donor and acceptor, insertion into the plasma membrane in intact cells may induce a basal conformation that result in high BRET signal, even in the non-activated state. Ligand binding may induce changes in both the distance and the relative orientation between the two partners, and the resulting BRET signal may be not significantly affected. Alternatively, high basal BRET signal in living cells may reflects autonomous, ligand-independent autophosphorylation/dephosphorylation activity of the insulin receptor in intact cells. This futile cycle will be lost with partially purified receptors, since in vitro BRET experiments, which are

Table 1 – EC_{50} for ligand-induced conformational change within homodimeric and hybrid receptors

Receptors	EC_{50} (nM)		
	Insulin	IGF-1	IGF-2
IRB-Rluc/IRB-YFP	1.12 ± 0.05	> 50	24.95 ± 0.06
IRB-Rluc/IRA-YFP	1.23 ± 0.09	> 50	$10.22 \pm 0.08^{**}$
IRA-Rluc/IRB-YFP	0.99 ± 0.14	> 50	$9.87 \pm 0.16^{**}$
IRA-Rluc/IRA-YFP	0.89 ± 0.12	24.97 ± 0.17	$9.77 \pm 0.21^{***}$

Results obtained in figure 7 were used to determine EC_{50} values using GraphPad Prism by curve fitting using sigmoidal dose response model. Results are the means ± S.E.M. of three independent experiments. $^{**}p < 0.01$; $^{***}p < 0.001$ when compared to EC_{50} of IGF-2 for IRB-Rluc/IRB-YFP receptor.

performed in absence of ATP, only reveal ligand-induced conformational changes, independently of any phosphorylation of the receptor. These and other possible mechanisms are presently under investigation in our laboratory.

In order to determine whether the homodimers and the hybrid receptors are pharmacologically different, we performed insulin, IGF-1 and IGF-2 dose-response experiments using partially purified receptors. The EC_{50} of insulin on homodimers and hybrid receptors are similar. In contrast, the EC_{50} of IGF-2 on IRA/IRB hybrid receptor and on IRA homodimer is 2.5-fold lower than on IRB homodimer. This result suggests that two symmetric high-affinity binding sites (one on each α-subunit) are not necessary for IGF-2 binding. In other words, one IGF-2 binding site on one subunit is sufficient to confer to the hybrid receptor IGF-2 binding properties similar to those of an IRA homodimer. A similar observation has been made previously for IGF1R/IRB hybrid receptor, which was able to bind IGF-2 with high-affinity, whereas IRB homodimer was not a high-affinity receptor for this ligand [14].

It has been shown previously that over-expression of IGF1R in breast cancer cells decreases insulin sensitivity through increased formation of IGF1R/IR hybrid receptors and thereby, decreased high-affinity binding sites for insulin [32]. Previous studies have also shown that the relative expression level of IRA and IRB isoforms can change in pathological situations such as diabetes and cancers [6–12]. These changes in IRA to IRB expression ratio should affect the proportion of homodimers and hybrid receptors at the cell surface. We have observed that the EC_{50} of IGF-2 is 2.5-fold higher for IRB homodimers than for IRA homodimers and IRA/IRB hybrids. In contrast, the EC_{50} of insulin on the three types of receptor are similar. These results suggest that an increase in the expression of one isoform relative to the other should not drastically affect the sensitivity of the cells to insulin but may modify their sensitivity to IGF-2. In cancer cells, an over-expression of IRA isoform has been observed. This over-expression has been suggested to increase IGFs signalling through increased IRA/IGF1R hybrid formation. Our work suggests that over-expression of IRA may also specifically increase IGF-2 signalling through increased formation of IRA/IRA homodimers and IRA/IRB hybrid receptors to the detriment of IRB/IRB homodimers.

In summary, in this work we have studied the hitherto uncharacterized IRA/IRB hybrid receptors. We have demonstrated that these hybrids are formed randomly in cells co-expressing both IR isoforms, and that they are capable of recruiting intracellular partners. Moreover, pharmacological characterization of IRA/IRB hybrids shows that no difference can be observed between the EC_{50} of insulin for hybrid receptors and for homodimers of each type, whereas the EC_{50} of IGF-2 is similar for hybrid receptors and for IRA homodimers, and is 2.5 higher for IRB homodimers. Because IGF-2 is implicated in progression of several cancers, IRA homodimers and IRA/IRB hybrid receptors may represent therapeutic targets for the treatment of cancer. The BRET-based assays developed in this work could be used to search for inhibitory molecules that are specific of these receptors.

Acknowledgements

This work was supported by the Association pour la Recherche sur le Cancer (Grant n° 3781). We thank Anne-Françoise Burnol for p52Shc cDNA and Stephano Marullo for Rluc-CD4 cDNA. We also thank Christian Frederici for useful discussion on statistical analysis methods and Nandy Simpson for critical reading of the manuscript.

Appendix A. Supplementary data

Supplementary data associated with this article can be found, in the online version, at doi:10.1016/j.bcp.2008.07.027.

REFERENCES

[1] Ebina Y, Ellis L, Jarnagin K, Edery M, Graf L, Clauser E, et al. The human insulin receptor cDNA: the structural basis for hormone-activated transmembrane signalling. Cell 1985;40:747–58.
[2] Seino S, Seino M, Nishi S, Bell GI. Structure of the human insulin receptor gene and characterization of its promoter. Proc Natl Acad Sci USA 1989;86:114–8.
[3] Moller DE, Yokota A, Caro JF, Flier JS. Tissue-specific expression of two alternatively spliced insulin receptor mRNAs in man. Mol Endocrinol 1989;3:1263–9.
[4] Mosthaf L, Grako K, Dull TJ, Coussens L, Ullrich A, McClain DA. Functionally distinct insulin receptors generated by tissue-specific alternative splicing. EMBO J 1990;9: 2409–13.
[5] Frasca F, Pandini G, Scalia P, Sciacca L, Mineo R, Costantino A, et al. Insulin receptor isoform A, a newly recognized, high-affinity insulin-like growth factor II receptor in fetal and cancer cells. Mol Cell Biol 1999;19:3278–88.
[6] Haring HU, Kellerer M, Mosthaf L. Modulation of insulin receptor signalling: significance of altered receptor isoform patterns and mechanism of hyperglycaemia-induced receptor modulation. Diabetologia 1994;37(Suppl. 2): S149–54.
[7] Mosthaf L, Vogt B, Haring HU, Ullrich A. Altered expression of insulin receptor types A and B in the skeletal muscle of non-insulin-dependent diabetes mellitus patients. Proc Natl Acad Sci USA 1991;88:4728–30.
[8] Sesti G, Marini MA, Tullio AN, Montemurro A, Borboni P, Fusco A, et al. Altered expression of the two naturally occurring human insulin receptor variants in isolated

adipocytes of non-insulin-dependent diabetes mellitus patients. Biochem Biophys Res Commun 1991;181:1419–24.
[9] Kellerer M, Sesti G, Seffer E, Obermaier-Kusser B, Pongratz DE, Mosthaf L, et al. Altered pattern of insulin receptor isotypes in skeletal muscle membranes of type 2 (non-insulin-dependent) diabetic subjects. Diabetologia 1993;36:628–32.
[10] Vella V, Pandini G, Sciacca L, Mineo R, Vigneri R, Pezzino V, et al. A novel autocrine loop involving IGF-II and the insulin receptor isoform-A stimulates growth of thyroid cancer. J Clin Endocrinol Metab 2002;87:245–54.
[11] Pandini G, Vigneri R, Costantino A, Frasca F, Ippolito A, Fujita-Yamaguchi Y, et al. Insulin and insulin-like growth factor-I (IGF-I) receptor overexpression in breast cancers leads to insulin/IGF-I hybrid receptor overexpression: evidence for a second mechanism of IGF-I signaling. Clin Cancer Res 1999;5:1935–44.
[12] Sciacca L, Costantino A, Pandini G, Mineo R, Frasca F, Scalia P, et al. Insulin receptor activation by IGF-II in breast cancers: evidence for a new autocrine/paracrine mechanism. Oncogene 1999;18:2471–9.
[13] Soos MA, Nave BT, Siddle K. Immunological studies of type I IGF receptors and insulin receptors: characterisation of hybrid and atypical receptor subtypes. Adv Exp Med Biol 1993;343:145–57.
[14] Benyoucef S, Surinya KH, Hadaschik D, Siddle K. Characterization of insulin/IGF hybrid receptors: contributions of the insulin receptor L2 and Fn1 domains and the alternatively spliced exon 11 sequence to ligand binding and receptor activation. Biochem J 2007;403:603–13.
[15] Bailyes EM, Nave BT, Soos MA, Orr SR, Hayward AC, Siddle K. Insulin receptor/IGF-I receptor hybrids are widely distributed in mammalian tissues: quantification of individual receptor species by selective immunoprecipitation and immunoblotting. Biochem J 1997;327(Pt 1):209–15.
[16] Federici M, Porzio O, Zucaro L, Fusco A, Borboni P, Lauro D, et al. Distribution of insulin/insulin-like growth factor-I hybrid receptors in human tissues. Mol Cell Endocrinol 1997;129:121–6.
[17] Federici M, Porzio O, Zucaro L, Giovannone B, Borboni P, Marini MA, et al. Increased abundance of insulin/IGF-I hybrid receptors in adipose tissue from NIDDM patients. Mol Cell Endocrinol 1997;135:41–7.
[18] Federici M, Zucaro L, Porzio O, Massoud R, Borboni P, Lauro D, et al. Increased expression of insulin/insulin-like growth factor-I hybrid receptors in skeletal muscle of noninsulin-dependent diabetes mellitus subjects. J Clin Invest 1996;98:2887–93.
[19] Boute N, Pernet K, Issad T. Monitoring the activation state of the insulin receptor using bioluminescence resonance energy transfer. Mol Pharmacol 2001;60:640–5.
[20] Blanquart C, Boute N, Lacasa D, Issad T. Monitoring the activation state of the insulin-like growth factor-1 receptor and its interaction with protein tyrosine phosphatase 1B using bioluminescence resonance energy transfer. Mol Pharmacol 2005;68:885–94.
[21] Blanquart C, Gonzalez-Yanes C, Issad T. Monitoring the activation state of insulin/insulin-like growth factor-1 hybrid receptors using bioluminescence resonance energy transfer. Mol Pharmacol 2006;70:1802–11.
[22] Boute N, Boubekeur S, Lacasa D, Issad T. Dynamics of the interaction between the insulin receptor and protein tyrosine-phosphatase 1B in living cells. EMBO Rep 2003;4:313–9.
[23] Lacasa D, Boute N, Issad T. Interaction of the insulin receptor with the receptor-like protein tyrosine phosphatases PTPalpha and PTPepsilon in living cells. Mol Pharmacol 2005;67:1206–13.
[24] Nouaille S, Blanquart C, Zilberfarb V, Boute N, Perdereau D, Roix J, et al. Interaction with Grb14 results in site-specific regulation of tyrosine phosphorylation of the insulin receptor. EMBO Rep 2006;7:512–8.
[25] Angers S, Salahpour A, Joly E, Hilairet S, Chelsky D, Dennis M, et al. Detection of beta 2-adrenergic receptor dimerization in living cells using bioluminescence resonance energy transfer (BRET). Proc Natl Acad Sci USA 2000;97:3684–9.
[26] Mercier JF, Salahpour A, Angers S, Breit A, Bouvier M. Quantitative assessment of beta 1- and beta 2-adrenergic receptor homo- and heterodimerization by bioluminescence resonance energy transfer. J Biol Chem 2002;277:44925–31.
[27] Ayoub MA, Levoye A, Delagrange P, Jockers R. Preferential formation of MT1/MT2 melatonin receptor heterodimers with distinct ligand interaction properties compared with MT2 homodimers. Mol Pharmacol 2004;66:312–21.
[28] Nouaille S, Blanquart C, Zilberfarb V, Boute N, Perdereau D, Burnol AF, et al. Interaction between the insulin receptor and Grb14: a dynamic study in living cells using BRET. Biochem Pharmacol 2006;72:1355–66.
[29] Soos MA, Field CE, Siddle K. Purified hybrid insulin/insulin-like growth factor-I receptors bind insulin-like growth factor-I, but not insulin, with high affinity. Biochem J 1993;290(Pt 2):419–26.
[30] Slaaby R, Schaffer L, Lautrup-Larsen I, Andersen AS, Shaw AC, Mathiasen IS, et al. Hybrid receptors formed by insulin receptor (IR) and insulin-like growth factor I receptor (IGF-IR) have low insulin and high IGF-1 affinity irrespective of the IR splice variant. J Biol Chem 2006;281:25869–74.
[31] Treadway JL, Morrison BD, Soos MA, Siddle K, Olefsky J, Ullrich A, et al. Transdominant inhibition of tyrosine kinase activity in mutant insulin/insulin-like growth factor I hybrid receptors. Proc Natl Acad Sci USA 1991;88:214–8.
[32] Zhang H, Pelzer AM, Kiang DT, Yee D. Down-regulation of type I insulin-like growth factor receptor increases sensitivity of breast cancer cells to insulin. Cancer Res 2007;67:391–7.